Chemistry Central Journal

RESEARCH ARTICLE Open Access

Correlation between Fischer-Tropsch catalytic activity and composition of catalysts

Sardar Ali[1], Noor Asmawati Mohd Zabidi[2*] and Duvvuri Subbarao[1]

Abstract

This paper presents the synthesis and characterization of monometallic and bimetallic cobalt and iron nanoparticles supported on alumina. The catalysts were prepared by a wet impregnation method. Samples were characterized using temperature-programmed reduction (TPR), temperature-programmed oxidation (TPO), CO-chemisorption, transmission electron microscopy (TEM), field emission scanning electron microscopy (FESEM-EDX) and N_2-adsorption analysis. Fischer-Tropsch synthesis (FTS) was carried out in a fixed-bed microreactor at 543 K and 1 atm, with H_2/CO = 2 v/v and space velocity, SV = 12L/g.h. The physicochemical properties and the FTS activity of the bimetallic catalysts were analyzed and compared with those of monometallic cobalt and iron catalysts at similar operating conditions.

H_2-TPR analysis of cobalt catalyst indicated three temperature regions at 506°C (low), 650°C (medium) and 731°C (high). The incorporation of iron up to 30% into cobalt catalysts increased the reduction, CO chemisorption and number of cobalt active sites of the catalyst while an opposite trend was observed for the iron-riched bimetallic catalysts. The CO conversion was 6.3% and 4.6%, over the monometallic cobalt and iron catalysts, respectively. Bimetallic catalysts enhanced the CO conversion. Amongst the catalysts studied, bimetallic catalyst with the composition of 70Co30Fe showed the highest CO conversion (8.1%) while exhibiting the same product selectivity as that of monometallic Co catalyst. Monometallic iron catalyst showed the lowest selectivity for C_{5+} hydrocarbons (1.6%).

1. Background

Fischer-Tropsch synthesis (FTS) is a process which deals with the conversion of syngas derived from coal, biomass and natural gas into hydrocarbons consisting of paraffins, olefins, alcohols and aldehydes with a high cetane number and is environmentally friendly [1]. Due to limited petroleum reserves and environmental restrictions, Fischer-Tropsch synthesis (FTS) is gaining more attention nowadays than ever. FTS is considered as a surface-catalyzed polymerization reaction. During this process, CO is adsorbed on the surface of the transition metal and hydrogenated producing CH_x monomers which consequently propagate to produce hydrocarbons and oxygenates with a broad range of functionalities and chain lengths [2].

All the group VIII elements show considerable activity for this process. Among them Co, Fe and Ru present the highest activity [3]. Due to high activity for Fischer-Tropsch synthesis, high selectivity to linear products, more stability towards deactivation, low activity towards water-gas shift (WGS) reaction and low cost compared to Ru, cobalt-based catalysts are the preferred catalyst for Fischer-Tropsch synthesis [4,5]. In order to enhance the catalytic activity and stability, different combinations of these active metals have been reported such as Co-Fe [6], Co-Mn [7] and Fe-Mn [8]. It has been reported that the addition of two active FTS metals gave additional properties which are quite different than the one expected for monometallic catalysts. The physical and chemical properties of Co/Fe systems have been discussed by Guerrero-Ruiz *et al.* [9]. In many heterogeneous reactions, these active phases are dispersed on a support which not only acts as a carrier but may also contribute to the catalytic activity. Al_2O_3, SiO_2 and TiO_2 are the commonly used supports for cobalt-based catalysts [10,11].

The incorporation of a second metal component into the catalyst may result in the geometric or electronic

* Correspondence: noorasmawati_mzabidi@petronas.com.my
[2]Department of Fundamental and Applied Sciences, Universiti Teknologi PETRONAS, Bandar Seri Iskandar, 31750 Tronoh, Perak, Malaysia
Full list of author information is available at the end of the article

modifications of the catalyst which may result in the modification of adsorption characteristics of the catalysts' surface and in some cases alter the reduction and deactivation behavior. Bimetallic catalysts possess different physicochemical properties than that of the monometallic catalysts. Pena O'Shea *et al*. [12] studied the activity of Co-Fe/SiO_2 in a fixed-bed and slurry reactors. They reported that bimetallic catalysts were more active and stable than the monometallic catalysts in the fixed-bed reactor. An opposite behavior was observed for the slurry reactor. The performance of Co-Fe/TiO_2 [13] catalyst has also been reported. The performance of the bimetallic on alumina has not that much been reported in the literature.

In this paper we wish to report our preliminary study on the synthesis of mono- and bimetallic catalysts of Co and Fe. The effects of incorporating Fe into Co on the physicochemical properties of the alumina-supported catalysts in terms of degree of reduction, CO and H_2 chemisorptions, metal particle size, textural properties and their selectivities and activities in the FTS are presented.

2. Results and Discussion

2.1 Morphology of catalysts

Figure 1 depicts the representative FESEM image of calcined Co/Al_2O_3 catalyst. The metal particles are indicated by arrows. FESEM analysis revealed that the metal particles were evenly distributed on the alumina support. Addition of iron in lower amounts (up to 30%) did not change the morphology of the catalysts. Figure 2 shows the TEM images of monometallic and bimetallic catalysts on Al_2O_3 support. The average size of metal-oxide particles was calculated from the TEM images. The average particle size of Co and Fe was found to be 13 nm and 10 nm, respectively. Incorporation of iron into Co resulted in an increase in the average metal particle size where for the 50Co50Fe on Al_2O_3, the average size of metal particles was found to be 18 nm.

2.2 Textural properties of the catalysts

BET specific surface area, total pore volume and average pore diameter of the samples are listed in Table 1. All the samples exhibited type IV isotherm at high relative pressures (p/po), which is typical of mesoporous materials. There was a significant decrease in BET specific surface area and pore volume for alumina after metal impregnation. The specific surface area of alumina was found to be 190 m^2/g while its pore volume was 0.1 cm^3/g with a pore diameter of 9.8 nm. The surface area of Co/Al_2O_3 and Fe/Al_2O_3 was 180 m^2/g and 165 m^2/g, respectively. Pore volume and pore size of these catalyst samples were found to be less than those of the alumina. The decrease in BET specific surface area, total pore volume and pore diameter after the impregnation

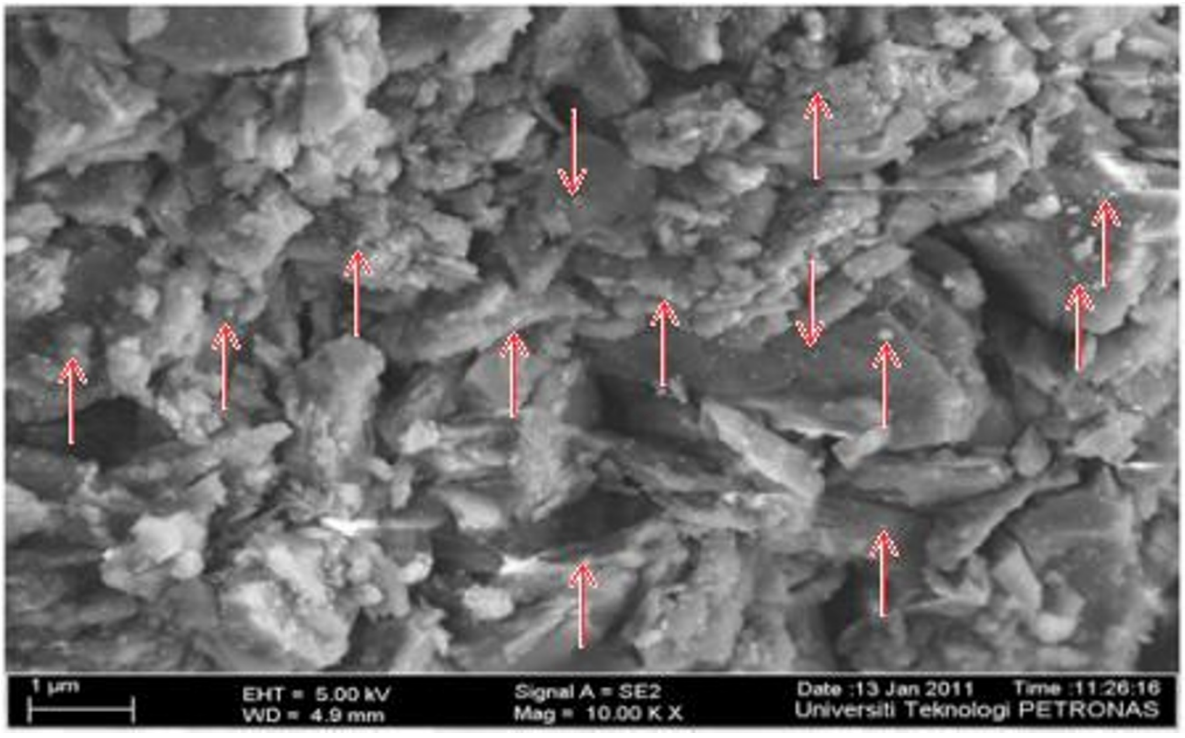

Figure 1 Representative FESEM image of the 5wt%Co/Al_2O_3 catalyst.

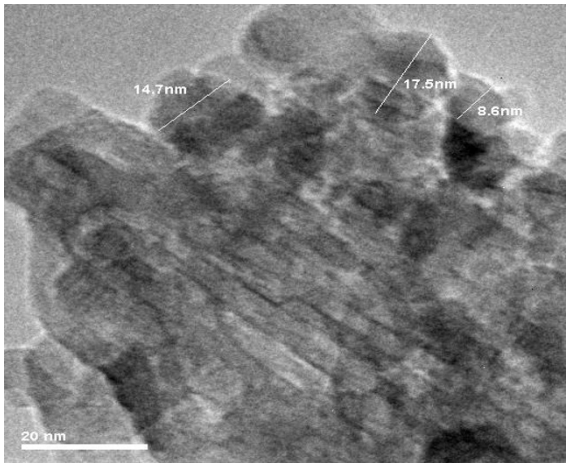

(a) Co/Al_2O_3

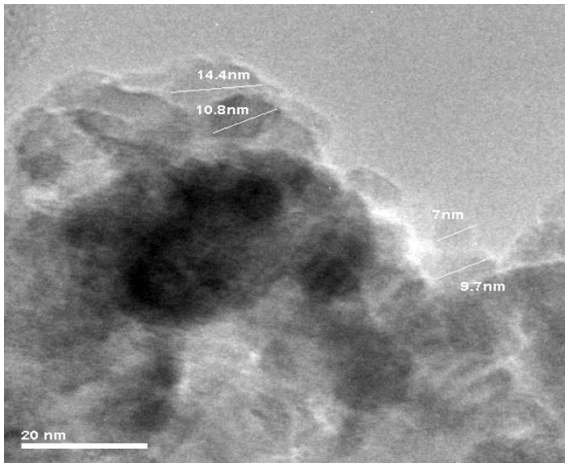

(b) Fe/Al_2O_3

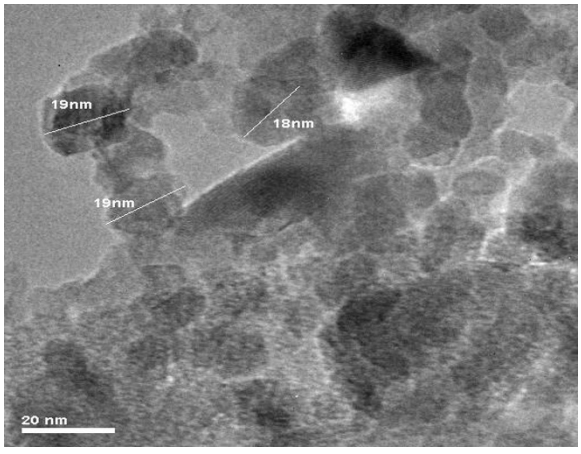

(c) $50Co50Fe/Al_2O_3$

Figure 2 TEM images of the catalyst 5wt% metal on Al_2O_3.

of metals on alumina indicated that metal nanoparticles were mainly incorporated inside the pores rather than on the external surface of alumina. This effect was even more pronounced for bimetallic catalysts as the Al_2O_3 surface area was reduced by 34%.

2.3 Reducibility of the catalysts

H_2-Temperature-programmed reduction (TPR) profiles of the catalysts are shown in Figure 3 and their peak positions are compiled in Table 2. For the Co/Al_2O_3 catalyst, the peak at 507°C was assigned to the first

Table 1 Textural data

Catalyst	BET surface area (m^2/g)	Total pore volume (cm^3/g)	Average pore diameter (nm)
γ-Al_2O_3	190	0.1	9.8
Co/Al_2O_3	180	0.08	7.5
Fe/Al_2O_3	165	0.07	6.7
$70Co30Fe/Al_2O_3$	127	0.07	6.4

reduction step of Co_3O_4 to CoO while the peak at 650°C was from the second reduction step of CoO to Co°. The peak appearing at 731°C was attributed to the reduction of very small metal particles and mixed metal-support oxides [14,15]. The reduction of iron oxides takes place in two steps. In the first step, Fe_2O_3 was reduced to Fe_3O_4 and the second step involved the reduction of Fe_3O_4 to FeO which was consequently reduced to Fe. Generally FeO is not expected to appear in the TPR spectra as it has been shown that FeO is unstable compared to Fe and Fe_3O_4. For the Fe/Al_2O_3,

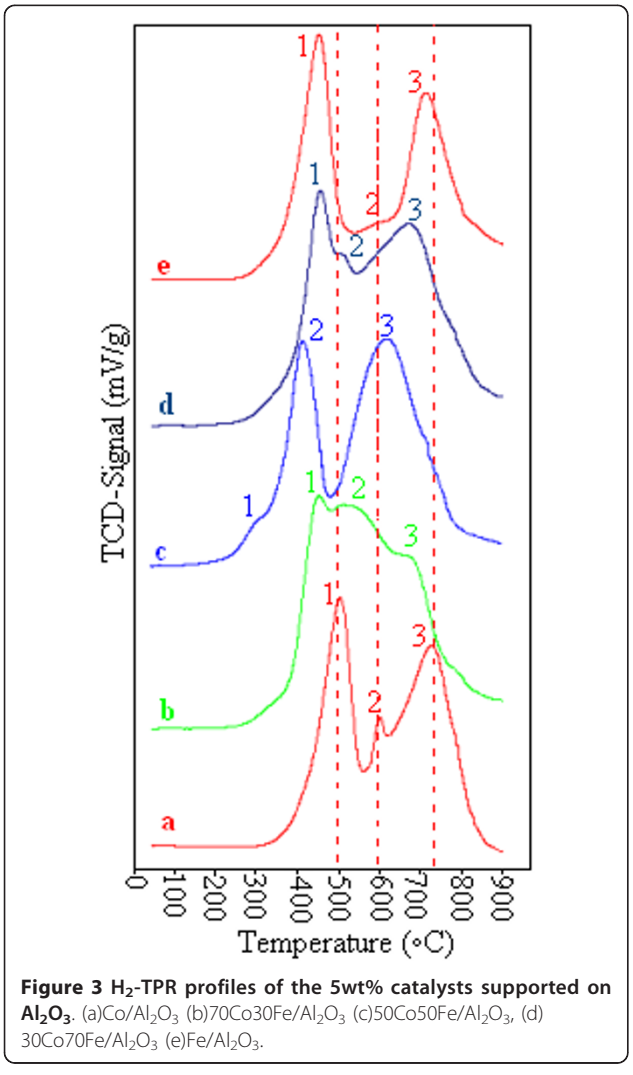

Figure 3 H_2-TPR profiles of the 5wt% catalysts supported on Al_2O_3. (a)Co/Al_2O_3 (b)$70Co30Fe/Al_2O_3$ (c)$50Co50Fe/Al_2O_3$, (d) $30Co70Fe/Al_2O_3$ (e)Fe/Al_2O_3.

reduction of Fe_2O_3 to Fe_3O_4 took place at 454°C. The reduction of Fe_3O_4 to Fe occurred at 635°C while the peak appearing at 716°C was assigned to the reduction of small metal particles and mixed oxides which are difficult to reduce [16,17].

Bimetallic catalysts showed different reduction patterns compared to monometallic catalysts. With the incorporation of iron, for $70Co30Fe/Al_2O_3$, the first reduction peak decreased from 507°C to 447°C while the second peak reduced from 650°C to 501°C and the third peak reduced from 731°C to 667°C. Similarly for the $50Co50Fe/Al_2O_3$ catalyst, reduction peaks decreased from 507°C, 650°C and 731°C to 328°C, 412°C and 614°C, respectively. With further increase in the iron content, for the $30Co70Fe/Al_2O_3$, the reduction temperatures increased again to 456°C, 458°C and 669°C, respectively. The same trend has also been reported in the literature [18].

The degree of reduction (D_{RT}) and the amounts of hydrogen consumed during TPR are given in Table 3. The degree of reduction (DRT), shown in Equation (1), is defined as the ratio of hydrogen consumed for the complete reduction of metal oxides from ambient temperature to 800°C to the amount of hydrogen calculated for this complete reduction [19].

$$DR_T(\%) = \frac{H_2 \text{ consumption } (\mu mol/g.cat)(\text{Peak 1 + Peak 2})}{\text{Total } H_2 \text{ consumption } (\mu mol/g.cat)} \quad (1)$$

As shown in Table 3, hydrogen consumption for monometallic Co/Al_2O_3 and Fe/Al_2O_3 was found to be 652.4 μmol/g.cat and 568.1 μmol/g.cat, respectively. Incorporation of iron into Co catalyst increased the hydrogen consumption, passing through a maximum for $50Co50Fe/Al_2O_3$ and then decreased with increasing iron loading.

For monometallic Co/Al_2O_3 and Fe/Al_2O_3, the degree of reduction was 58.2% and 52.4%, respectively. With the incorporation of iron into cobalt catalyst, for the $70Co30Fe/Al_2O_3$, the degree of reduction was 70.7%. With further increase in the amount of iron incorporated, a decrease in the degree of reduction was observed where for the $50Co50Fe/Al_2O_3$ and $30Co70Fe/Al_2O_3$ the degree of reduction was 34.6% and 40.1%, respectively. Based on the TPR analysis, it can be concluded that incorporation of 30% of iron into cobalt catalysts enhanced the reducibility, while iron-enriched

Table 2 H_2-TPR data of the catalysts

Catalysts	Reduction temperature (°C)		
	Peak 1	Peak 2	Peak 3
Co/Al_2O_3	507	650	731
$70Co30Fe/Al_2O_3$	447	501	667
$50Co50Fe/Al_2O_3$	328	412	614
$30Co70Fe/Al_2O_3$	456	458	669
Fe/Al_2O_3	454	635	716

catalysts displayed an opposite trend. This trend may be due to the fact that incorporation of Fe in higher amounts resulted in the formation of mixed-oxide phases, which were difficult to reduce. The formation of these mixed-oxide phases were confirmed by XRD analysis.

2.4 CO-Chemisorptions and O_2-Pulse re-oxidation

TPD and oxygen pulse re-oxidation (assuming Co^0 was completely oxidized to Co_30_4) techniques were used to calculate the % dispersion [18], % reduction [20] and number of active sites [21] of the catalysts, using equations (2), (3) and (4), respectively.

$$\%\,\text{reduction} = \frac{\text{O2 uptake} \times 2/3 \times \text{atomic weight}}{\text{percent metal}} \quad (2)$$

$$\%\,\text{dispersion} = \frac{\text{H2 uptake} \times \text{atomic weight} \times \text{stochiometry}}{\%\,\text{metal}} \quad (3)$$

$$\text{No. of active sites} = \frac{\text{wt. of Co in the sample} \times \text{reduction} \times \text{dispersion} \times N_A}{MW} \quad (4)$$

The results of CO chemisorptions and oxygen pulse re-oxidation for all the samples are summarized in Table 4. It was found that the amount of CO uptake for the Co/Al_2O_3 catalyst was 2.41 μmol/g, which doubled that of Fe/Al_2O_3 (1.27 μmol/g). With increasing content of iron incorporated into Co, the CO uptake decreased. For $30Co70Fe/Al_2O_3$, $50Co50Fe/Al_2O_3$, $70Co30Fe/Al_2O_3$, the CO uptake was 1.57 μmol/g, 2.50 μmol/g and 3.77 μmol/g, respectively.

As shown in Table 4, for the Co/Al_2O_3 catalyst the reduction was 13.2% while for monometallic Fe/Al_2O_3 it was found to be 8%. Incorporation of Fe into Co resulted in an increase in the reduction passing through a maximum for $70Co30Fe/Al_2O_3$. Incorporation of 30% Fe into cobalt catalyst increased the reduction by 53.5% while for the $50Co50Fe/Al_2O_3$ catalyst, the increase in the reduction was found to be 52%. Amongst the bimetallic catalysts, the $50Co50Fe/Al_2O_3$ catalyst exhibited lowest dispersion, which could be due to the formation of mixed-oxide phases which were difficult to reduce.

The dispersion of cobalt crystallites in the Co/Al_2O_3 catalyst was 4.2% while Fe/Al_2O_3 exhibited a dispersion of 3.7%. The dispersion decreased significantly with iron incorporation, possibly due to the coverage of active sites of Co species by Fe atoms. The dispersion for the bimetallic $30Co70Fe/Al_2O_3$, $50Co50Fe/Al_2O_3$ and $70Co30Fe/Al_2O_3$ catalysts were 3.0%, 2.3% and 3.2% respectively. Incorporation of Fe into the cobalt catalysts resulted in an increase in the number of active sites of the metal. The increase in the number of active sites for the catalysts followed the same trend as that for reduction and dispersion passing through a maximum for the bimetallic $70Co30Fe/Al_2O_3$ catalyst. Incorporation of Fe up to 30% into the cobalt catalyst resulted in an increase in the reduction and consequently the number of active sites increased.

2.5 XRD analysis

The crystal phases of the Al_2O_3 support and supported monometallic and bimetallic catalysts after calcinations are shown in Figure 4. In the XRD spectrum of alumina support and all catalysts, peaks at 2θ values of 46° and 66° correspond to that of gamma alumina [3]. The monometallic Co/Al_2O_3 sample displayed the diffraction lines of Co_3O_4 spinel at 2θ values of 28.5°, 34°, 35.5°, 42°, 53°, 62.5° and 66° [13,22,23]. Monometallic Fe/Al_2O_3 sample exhibited the pattern of hematite at 2θ values of 16°, 28.5°, 35°, 44°, 51°, 56.5° and 61°. For all the bimetallic catalysts, along with characteristic diffraction patterns of Co_3O_4 and Fe_2O_3, diffraction patterns of $CoFe_4O_4$ also appeared at 2θ values of 16°, 35°, 43°, 53°, 56.5° and 61° [13,22,23]. The appearance of diffraction patterns of $CoFe_4O_4$ confirmed the formation of complex mixed oxides phases of iron and cobalt. The formation of these mixed-oxide phases may be responsible for the decrease in the reducibility

Table 3 Total H_2-consumption and degree of reduction of the catalysts

Catalysts	H_2-Consumption (μmol/g.cat)				Degree of reduction (%)		$^{\#}DR_T$(%)
	Peak 1	Peak 2	Peak 3	Total	Peak 1	Peak 2	
Co/Al_2O_3	260.9	117	377.9	652.4	40.12	18.1	58.2
$70Co30Fe/Al_2O_3$	188.2	325.3	212.5	728.9	25.9	44.8	70.7
$50Co50Fe/Al_2O_3$	43.9	232.3	521.71	798.1	5.51	29.12	34.6
$30Co70Fe/Al_2O_3$	159.8	60.4	329.1	549.3	29.1	11.01	40.1
Fe/Al_2O_3	258	38.8	271.6	568.1	45.4	6.84	52.4

Table 4 Dispersion and reduction percentages of the catalysts

Catalysts	O_2-Chemisorbed (μmol/g.cat)	CO-Chemisorbed (μmol/g.cat)	Reduction (%)	Dispersion (%)	No.of active sites ($\times 10^{19}$)
Co/Al_2O_3	80.8	2.41	13.2	4.2	2.8
$70Co30Fe/Al_2O_3$	180.4	3.77	28.4	3.2	4.5
$50Co50Fe/Al_2O_3$	177.0	2.50	27.8	2.3	3.3
$30Co70Fe/Al_2O_3$	83.2	1.57	13.0	3	2.0
Fe/Al_2O_3	50.2	1.27	8.0	3.7	1.5

of the $50Co50Fe/Al_2O_3$ bimetallic catalysts, as shown in the TPR profiles.

2.6 Activity and selectivity

The catalytic activity and product selectivity data were calculated after 5 hours of time on stream. The CO conversions and product selectivities over the monometallic and bimetallic catalysts are summarized in Table 5. The CO conversion of 6.3% and 4.6% was obtained over Co/Al_2O_3 and Fe/Al_2O_3, respectively. The incorporation of Fe into Co resulted in an increase in the CO conversion passing through a maximum for the $70Co30Fe/Al_2O_3$. The values of CO conversion for bimetallic catalysts $70Co30Fe/Al_2O_3$, $50Co50Fe/Al_2O_3$ and $30Co70Fe/Al_2O_3$ were 8.1%, 7.5% and 4.2%, respectively. This trend was in accordance with the results of catalyst characterizations. Incorporation of Fe up to 30% into the Co catalysts led to higher reducibility which in turn resulted in more metal active sites available for Fischer-Tropsch synthesis and thus enhanced catalytic activity. The highest CO conversion was achieved using the $70Co30Fe/Al_2O_3$ which also had the highest CO adsorption capacity. Figure 5 shows variation of CO conversion and number of active sites as a function of catalysts' compositions. Incorporation of iron up to 30% resulted in an increase in the number of metal active sites and hence the increase in CO conversion. Further increase in the amount of iron decreased the number of active sites and hence the CO conversion.

Using the Co/Al_2O_3 catalyst, selectivity for methane, light hydrocarbons and C_{5+} were 15.6%, 80.9% and 3.5%, respectively. A monometallic Fe/Al_2O_3 catalyst was more selective to methane and lower hydrocarbons than C_{5+} where selectivities to methane, light hydrocarbons and C_{5+} were 27.5%, 70.9% and 1.6%, respectively. With the addition of 30% of Fe into cobalt, the CO conversion increased but the product distribution was similar to that of the monometallic Co/Al_2O_3. However, using the $50Co50Fe/Al_2O_3$ and $30Co70Fe/Al_2O_3$ catalysts, the methane selectivity increased by a factor 15.3% and 19%, respectively whereas the C_{5+} selectivity decreased by 37.2% and 71.4%, respectively.

The C_2-C_5 hydrocarbon fractions were included in the olefinity calculation. As shown in Table 5, incorporation of Fe into Co changed the olefin to paraffin ratios of the products. Olefinity of the Fe-based catalysts was higher (1.04) than that of Co-based catalyst (0.41). For bimetallics $70Co30Fe/Al_2O_3$, $50Co50Fe/Al_2O_3$ and $30Co70Fe/Al_2O_3$, the increase in olefin to paraffin ratio was 29.2%, 56% and 78%, respectively compared to that of monometallic Co/Al_2O_3.

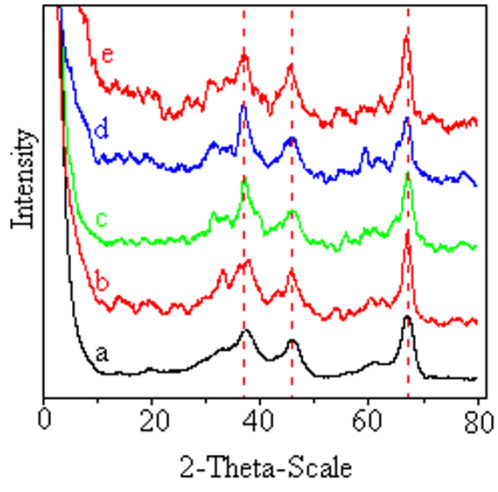

Figure 4 XRD spectra. (a) γ-Al_2O_3(b) Co/Al_2O_3(c) $70Co30Fe/Al_2O_3$(d) $50Co50Fe$(e) Fe/Al_2O_3.

3. Conclusions

Alumina-supported monometallic Co and Fe and a series of Fe/Co bimetallic catalysts were studied. The Fe/Co bimetallic exhibited different physicochemical properties than the monometallic Co and Fe catalysts. Various characterization techniques revealed that addition

Table 5 Activity and product distribution data for the Al_2O_3-supported catalysts

Catalysts	% CO conversion	Product selectivity (%)			Olefinity
		C_1	C_2-C_4	C_{5+}	
Co/Al_2O_3	6.3	15.6	80.9	3.5	0.41
$70Co30Fe/Al_2O_3$	8.1	16.1	80.7	3.2	0.53
$50Co50Fe/Al_2O_3$	7.5	18.4	79.4	2.2	0.64
$30Co70Fe/Al_2O_3$	4.2	19.0	80.0	1.0	0.73
Fe/Al_2O_3	4.6	27.5	70.9	1.6	1.04

FT reaction conditions: P = 1 atm, T = 543 K, H_2/CO = 2 v/v, space velocity (SV) = 12 L/g.h.

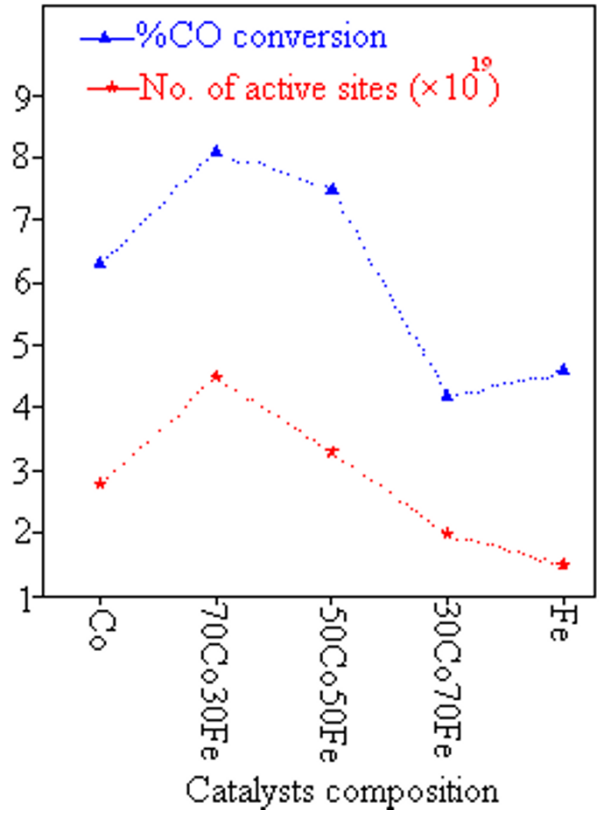

Figure 5 Correlation between the catalysts' compositions and the number of active sites and CO conversions.

of Fe up to 30% resulted in an enhanced reducibility and increase in the CO and hydrogen chemisorptions which resulted in an increase in the number of active sites and consequently increased the CO conversion by 28%. However hydrocarbons selectivities did not change significantly. Further increase in Fe resulted in increasing trend in CH_4 selectivity and decreasing C_{5+} selectivity which could be due to the formation of bimetallic mixed oxides phases, enriched with Fe.

4. Experimental

Preparation of catalysts

All the monometallic and bimetallic nanocatalysts were prepared using the wet impregnation method with 5wt% metal loading. These catalysts were assigned as 5wt%(X%:Y%)/Alumina (where X% and Y% represent percentage of Co and Fe, respectively). Before impregnation, alumina (Merck, BET 190 m^2/g) was calcined at 500°C for 6 hours. For each catalyst, required amounts of the precursor salts i.e. Co $(NO_3)_2.6H_2O$ (≥ 98%, Fluka) and $Fe(NO_3)_3.9H_2O$ (≥ 99.0%, Merck) were dissolved in deionized water and added to the support drop-wise with constant stirring followed by drying in an oven at 120°C overnight and calcining at 500°C in nitrogen atmosphere for 6 hours.

Characterization of catalysts

The reduction behavior of the catalysts was studied using TPDRO1100 MS (CE instrument) equipped with a thermal conductivity detector and a mass spectrometer. The catalyst sample (0.5 g) was placed in a U-shaped quartz tube and degassed in a flow of nitrogen at 200°C to remove traces of water. Temperature-programmed reduction (TPR) was performed using 5% H_2/N_2 with a flow rate of 20 cm^3min^{-1} and heating from 40°C to 900°C at 10°C min^{-1}. For CO and H_2 chemisorptions, 25 mg of the calcined catalyst was reduced under hydrogen flow at 400°C for 5 h and then cooled to 50°C. Then the flow of hydrogen was switched to nitrogen. Temperature-programmed desorption (TPD) of the sample was performed by increasing the temperature of the sample to 400°C at 10°C min^{-1} under argon flow. The TPD spectra were used to calculate the metal dispersion. After the H_2-TPD, sample was re-oxidized by pulses of 10% Oxygen in helium (TPO). The resultant TPO spectra were used to determine the % reduction. The CO chemisorption was performed by introducing pulses of pure CO at 250°C after the H_2-TPD. Morphology of the catalyst sample was characterized using transmission electron microscopy (Zeiss LIBRA 200 TEM) at 200 kV accelerating voltage. The surface area, pore volume and average pore size distribution of the catalyst samples were measured using N_2-adsorption (Micromeritics, ASAP 2020). Crystallinity of the samples were measured by powder X-ray diffraction (XRD), using a Bruker D8 Advance horizontal X-ray diffractometer equipped with a Cu anode.

Catalytic study

Fischer-Tropsch reaction was performed in a fixed bed microreactor at 543 K and 1 atm with H_2/CO = 2 v/v and space velocity, SV = 12 L/g.h. Typically 0.03 gm of calcined catalyst sample was reduced in situ at 653 K for 5 h in 30 ml min^{-1} of pure hydrogen. On-line gas analysis was performed during the FTS reaction using Agilent 6890 Hewlett Packard (HP) gas chromatograph (GC) equipped with TCD and FID detectors. The CO conversion, hydrocarbon (HC) selectivity and olefinity were calculated using equation (5), (6) and (7), respectively.

$$\text{CO conversion}\,(\%) = \frac{\text{moles of CO}_{in} - \text{moles of CO}_{out}}{\text{moles of CO}_{in}} \times 100 \quad (5)$$

$$\text{HC selectivity}\,(\%) = \frac{\text{moles of HC produced}}{\text{total moles of HC}} \times 100 \quad (6)$$

$$\text{Olefinity} = \frac{\text{moles of olefin}}{\text{moles of paraffin}} \quad (7)$$

Acknowledgements
The authors acknowledged financial support provided by Ministry of Science, Technology and Innovation (E-Science Fund No: 03-02-02-SF0036), FRGS grant (project No: (FRGS/2/2010/SG/UTP/02/3) and Short Term Internal Fund Universiti Teknologi PETRONAS (Project No.31/09.10).

Author details
[1]Department of Chemical Engineering, Universiti Teknologi PETRONAS, Bandar Seri Iskandar, 31750 Tronoh, Perak, Malaysia. [2]Department of Fundamental and Applied Sciences, Universiti Teknologi PETRONAS, Bandar Seri Iskandar, 31750 Tronoh, Perak, Malaysia.

Authors' contributions
SA performed the experiments and drafted the manuscript. DS assisted in the Fischer-Tropsch reaction study. NAMZ participated in the conception, design of study and revision of the manuscript. All authors read and approved the final manuscript.

Competing interests
The authors declare that they have no competing interests.

Received: 10 August 2011 Accepted: 3 November 2011
Published: 3 November 2011

References

1. Dry ME: **Fischer-Tropsch reactions and the environment.** *Appl Catal A* 1999, **189**:185-190.
2. Brady RC, Pettit R: **Reactions of diazomethane on transition-metal surfaces and their relationship to the mechanism of the Fischer-Tropsch reaction.** *J Am Chem Soc* 1980, **102**:6181-6182.
3. Tavasoli A, Mortazavi Y, Khodadadi A, Sadagiani K: **Effects of different loadings of Ru and Re on physico-chemical properties and performance of 15% Co/Al_2O_3 FTS catalysts.** *Iran J Chem Che Eng* 2005, **35**:9-15.
4. Iglesia E: **Design, synthesis, and use of cobalt-based Fischer-Tropsch synthesis catalysts.** *Appl Catal A* 1997, **161**:59-78.
5. Khodakov AY, Chu W, Fongarland P: **Advances in the development of novel cobalt Fischer-Tropsch catalysts for synthesis of long-chain hydrocarbons and clean fuels.** *Chem Rev* 2007, **5**:1692-1744.
6. Arcuri KB, Schwartz H, Pitrowski RD, Butt JB: **Iron alloy Fischer-Tropsch catalysts: IV. Reaction and selectivity studies of the FeCo system.** *J Catal* 1985, **85**:349-361.
7. Morales Cano F, Gijzeman OLJ, de Groot FMF, Weckhuysen BM: **Manganese promotion in cobalt-based Fischer-Tropsch catalysis.** *Stud in Surf Sci Catal* 2004, **147**:271-276.
8. Yang Y, Xiang H, Zhang R, Zhong B, Li Y: **A highly active and stable Fe-Mn catalyst for slurry Fischer-Tropsch synthesis.** *Catal Today* 2005, **106**:170-175.
9. Guerrero-Ruiz , Septilueda-Escribano A, Rodriguez-Ramos I: **Carbon supported bimetallic catalysts containing iron: Preparation and characterization.** *Appl Catal A* 1992, **81**:81-100.
10. Berge PJ, Loosdrecht VJ, Barradas S, Kraan AM: **Oxidation of cobalt based Fischer-Tropsch catalysts as a deactivation mechanism.** *Catal Today* 2000, **58**:321-334.
11. Jacobs G, Das TK, Zhang Y, Li J, Racoillet G, Davis BH: **Fischer-Tropsch synthesis: support, loading, and promoter effects on the reducibility of cobalt catalysts.** *Appl Catal A* 2002, **233**:263-281.
12. de la Pena OShea VA, Álvarez-Galvana MC, Campos-Martín JM, Fierro JLG: **Fischer-Tropsch synthesis on mono- and bimetallic Co and Fe catalysts in fixed-bed and slurry reactors.** *Appl Catal A* 2007, **326**:65-73.
13. Duvenhage DJ, Coville NJ: **$CoFe/TiO_2$ bimetallic catalysts for the Fischer-Tropsch reaction I. Characterization and reactor studies.** *Appl Catal A* 1997, **153**:43-67.
14. Kozhuharova R, Ritschel M, Elefant D, Graff A, Monch I, Muhl T, Schneider CM, Leonhardt A: **(Fe_xCo_{1-x})-alloy filled vertically aligned carbon nanotubes grown by thermal chemical vapor deposition.** *J Mag Magnetic Mater* 2005, **290-291**:250-253.
15. Jacobs G, Chaney JA, Patterson PM, Das TK, Davis BH: **Fischer-Tropsch synthesis: Study of the promotion of Re on the reduction property of Co/Al_2O_3 catalysts by in situ EXAFS/XANES of Co K and Re LIII edges and XPS.** *Appl Catal A* 2004, **264**:203-212.
16. Kock AJ, Fortuin HM, Geus JW: **The reduction behavior of supported iron catalysts in hydrogen or carbon monoxide atmospheres.** *J Catal* 1985, **96**:261-275.
17. Lohitharn N, Goodwin JG, Lotero E: **Impact of Cr, Mn and Zr addition on Fe Fischer-Tropsch synthesis catalysis: Investigation at the active site level using SSITKA.** *J Catal* 2008, **255**:104-113.
18. Duvenhage DJ, Coville NJ: **$CoFe/TiO_2$ bimetallic catalysts for the Fischer-Tropsch reaction I. Characterization and reactor studies.** *Appl Catal A* 1997, **153**:43-67.
19. Abbaslou RM, Tavasoli A, Dalai AK: **Effect of Pre-treatment on Physico-Chemical Properties and Stability of Carbon Nanotubes Supported Iron Fischer-Tropsch.** *Appl Catal A* 2009, **355**:33-41.
20. Tavasoli A, Sadagiani K, Khorashe F, Seifkordi A, Rohani A, Nakhaeipour A: **Cobalt supported on carbon nanotubes-A promising novel Fischer-Tropsch synthesis catalyst.** *Fuel Process Tech* 2008, **89**:491-498.
21. Tavasoli A: **Catalyst composition and its distribution effects on the enhancement of activity, selectivity and suppression of deactivation rate of FTS cobalt catalysts.** Ph.D. Thesis, University of Tehran: Tehran, Iran; 2005.
22. de la Pena OShea VA, Menendez N, Tornero JD, Fierro JLG: **Unusually high selectivity to C2+ alcohols on bimetallic CoFe catalysts during CO hydrogenation.** *Catal Lett* 2003, **88**:123-128.
23. Tihay F, Pourroy G, Richard-Plouet M, Roger AC, Kiennemann A: **Effect of Fischer-Tropsch synthesis on the microstructure of Fe-Co-based metal/spinel composite materials.** *Appl Catal A* 2001, **206**:29-42.

doi:10.1186/1752-153X-5-68
Cite this article as: Ali *et al.*: Correlation between Fischer-Tropsch catalytic activity and composition of catalysts. *Chemistry Central Journal* 2011 **5**:68.